Electronic Supplementary Information (ESI):

Lanthanoid Single-Ion Magnets with LnN_{10} Coordination Geometry

Zhong-Xia Jiang,‡ Jun-Liang Liu,‡ Yan-Cong Chen, Jiang Liu, Jian-Hua Jia* and Ming-Liang Tong*

MOE Key Lab of Bioinorganic and Synthetic Chemistry, School of Chemistry & Chemical Engineering, Sun Yat-Sen University, Guangzhou 510275, P. R. China.

E-mail: jiajh3@mail.sysu.edu.cn; tongml@mail.sysu.edu.cn.

‡ These authors contributed equally to this work.

CONTENT:

EXPERIMENTAL SECTION

Materials and Physical Measurements. The ligand was synthesized as literature described.[1] Metal salts and other reagents were commercially available and used as received without further purification. The C, H, N and S microanalyses were carried out with an Elementar Vario-EL CHNS elemental analyzer. X-ray powder diffraction (XRPD) intensities for polycrystalline samples were measured at 293 K on Bruker D8 Advance Diffratometer (Cu-K_α, λ = 1.54056 Å) by scanning over the range of 5-50° with step of 0.2°/s. Calculated patterns were generated with Mercury. The luminescence spectra were measured using an Edinburgh Instrument FLS980 Combined Fluorescence Lifetime and Steady State Spectrometer. The steady-state luminescence was excited by unpolarized light from a 450 W xenon CW lamp at 298 K and 15 K. The lifetime measurements were excited by a pulsed μs flash lamp at 298 K. Magnetic susceptibility measurements were performed with a Quantum Design MPMS-XL7 SQUID. Polycrystalline samples were embedded in vaseline to prevent torquing. Data were corrected for the diamagnetic contribution calculated from Pascal constants.

X-ray Structure Determination. Diffraction intensities were collected on a Rigaku R-AXIS SPIDER IP diffractometer with Mo Kα radiation (λ = 0.71073 Å) for complexes **1** and **2** at 150(2) K. The structures were solved by direct methods, and all non-hydrogen atoms were refined anisotropically by least-squares on F^2 using the SHELXTL program suite.[2] Anisotropic thermal parameters were assigned to all non-hydrogen atoms. The hydrogen atoms attached to carbon, nitrogen and oxygen atoms were placed in idealised positions and refined using a riding model to the atom to which they were attached. The disordered solvent molecules were squeezed[3] and reconfirmed by the elemental analysis. CCDC 1426946 (**1**) and 1426947 (**2**) contain the supplementary crystallographic data for this paper. These data can be obtained free of charge via www.ccdc.cam.ac.uk/conts/retrieving.html.

Synthesis. $Dy(\mathbf{N_5})_2(CF_3SO_3)_3$ (**1**): A mixture of 2,6-diacetyl pyridine (0.10 mmol) and 2-diazanyl pyridine (0.20 mmol) was dissolved in 6 mL acetonitrile. Under stirring, the solution was turned yellow. After 30 minutes, $Dy(CF_3SO_3)_3$ (0.05 mmol) was added and the mixture was stirred for 30 minutes. Yellow crystals suitable for X-ray analysis were obtained in several days by slow diffusion of diethyl ether into the solution above. Elemental analysis (%) for $C_{41}H_{38}DyF_9N_{14}O_9S_3$, calcd, C: 37.87, H: 2.95, N: 15.08, S: 7.40; found, C: 37.77, H: 3.02, N: 15.22, S: 7.37.

$Dy(\mathbf{N_5})_2(CF_3SO_3)_3$ (**2**): the procedure was the same as that employed for complex **1**, except that pyridine was replaced by metal salts. The yellow crystals were obtained by slow diffusion of diethyl ether into the solution. Elemental analysis (%) for $C_{41}H_{38}ErF_9N_{14}O_9S_3$, calcd, C: 37.73, H: 2.93, N: 15.02, S: 7.37; found, C: 38.16, H: 3.10, N: 15.34; S: 7.22.

Reference:

[1] J. D. Curry, M. A. Robinson and D. H. Busch, *Inorg. Chem.*, 1967, **6**, 1570.

[2] G. M. Sheldrick, *Acta Crystallogr.*, 2008, **A64**, 112.

[3] P. van der Sluis and A. L. Spek, *Acta Crystallogr.*, 1990, **A46**, 194.

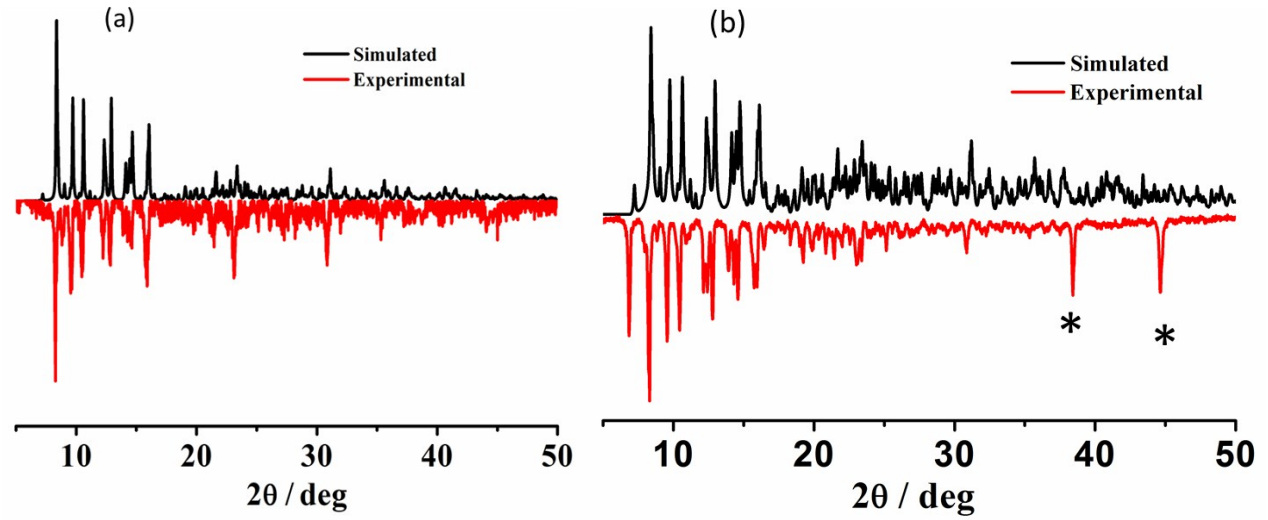

Figure S1. Experimental and simulated powder X-ray diffraction (PXRD) patterns for **1** (*a*) and **2** (*b*). The peaks marked with * were due to silicon carrier.

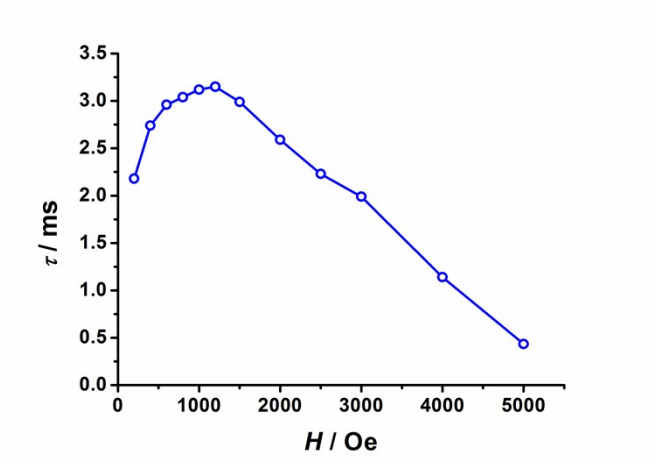

Figure S2. The dc field dependence of the relaxation time for **1** at 1.8K. The solid line is a guide for the eye.

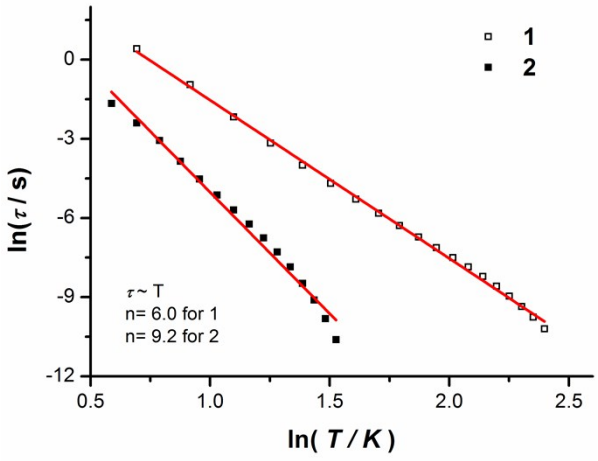

Figure S3. The plots of the relaxation time τ *vs*. T on a log-log scale for **1** and **2**. The red lines are for the best linear fitting.

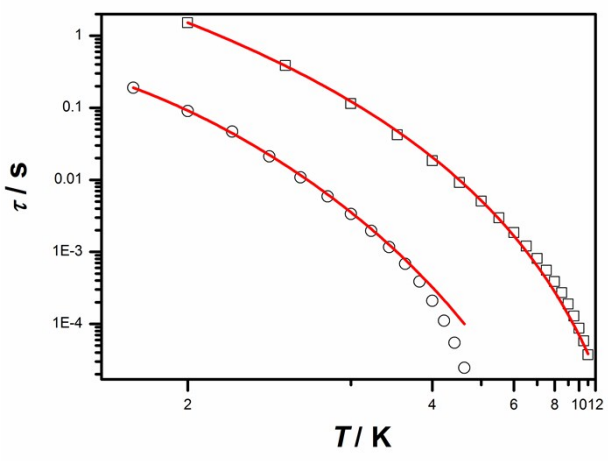

Figure S4. The plots of the relaxation time τ *vs*. T with consideration of the direct and Raman processes for **1** (*square*) and **2** (*circle*). The red lines are fitted with the equation: $\tau^{-1} = AT + BT^n$.

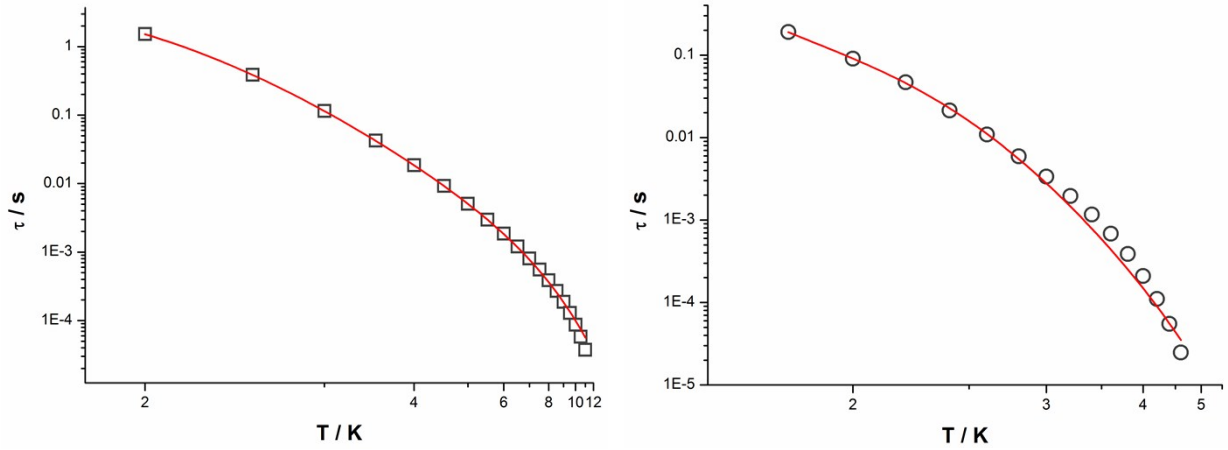

Figure S5. The plots of the relaxation time τ *vs*. T with consideration of the direct, Raman, and Obach processes for **1** (*square*) and **2** (*circle*). The red lines are fitted with the equation: $\tau^{-1} = AT + BT^n + \tau_0^{-1} \exp(-U_{eff}/k_B T)$.

Table S1. Crystallographic Data and Structural Refinements for **1** and **2**.

compound	**1**	**2**
Formula	$C_{41}H_{38}DyF_9N_{14}O_9S_3$	$C_{41}H_{38}ErF_9N_{14}O_9S_3$
M_r	1300.53	1305.29
Temp. */ K*	150(2)	150(2)
Crystal system	orthorhombic	orthorhombic
Space group	*Pbca*	*Pbca*
a / Å	20.8179(9)	20.6900(4)
b / Å	19.5864(10)	19.5456(5)
c / Å	24.4923(13)	24.4270(5)
α / Å	90	90
β / Å	90	90
γ / Å	90	90
V / Å^3	9986.7(9)	9878.2(4)
Z	8	8
$\rho_{calcd.}$ (g/cm^3)	1.730	1.755
μ (mm^{-1})	1.724	1.929
F (000)	5192.0	5208.0
Reflns obsd [$I \geq 2\sigma(I)$]	9543	9543
GOF on F^2	1.052	1.038
R_1 [$I \geq 2\sigma(I)$][a]	0.0649(6407)	0.0475(8890)
wR_2 (all data)[b]	0.1750(11325)	0.1200(10620)
CCDC No.	1426946	1426947

[a] $R_1 = \sum||F_o| - |F_c||/\sum|F_o|$. [b] $wR_2 = [\sum w(F_o^2 - F_c^2)^2/\sum w(F_o^2)^2]^{1/2}$.

Table S2. Selected bond lengths (Å) and bond angles (°) for **1**.

	Length(Å)		Length(Å)
Dy-N1	2.564(6)	Dy-N8	2.571(6)
Dy-N2	2.526(6)	Dy-N9	2.563(6)
Dy-N4	2.554(6)	Dy-N11	2.609(6)
Dy-N5	2.551(6)	Dy-N12	2.555(6)
Dy-N7	2.585(6)	Dy-N14	2.586(6)
	Angle(°)		Angle(°)
N1-Dy-N2	61.3(2)	N4-Dy-N14	73.6(2)
N1-Dy-N4	112.9(2)	N5-Dy-N7	60.82(19)
N1-Dy-N5	61.71(18)	N5-Dy-N8	117.15(18)
N1-Dy-N7	112.72(19)	N5-Dy-N9	135.14(19)
N1-Dy-N8	178.75(17)	N5-Dy-N11	85.06(19)
N1-Dy-N9	119.64(19)	N5-Dy-N12	74.12(19)
N1-Dy-N11	68.39(19)	N5-Dy-N14	76.8(2)
N1-Dy-N12	117.7(2)	N7-Dy-N8	66.63(18)
N1-Dy-N14	67.75(19)	N7-Dy-N9	82.21(18)
N2-Dy-N4	61.5(2)	N7-Dy-N11	74.80(19)
N2-Dy-N5	123.0(2)	N7-Dy-N12	75.54(19)
N2-Dy-N7	147.68(18)	N7-Dy-N14	125.76(19)
N2-Dy-N8	119.82(19)	N8-Dy-N9	61.46(19)
N2-Dy-N9	75.7(2)	N8-Dy-N11	112.2(2)
N2-Dy-N11	73.76(19)	N8-Dy-N12	61.2(2)
N2-Dy-N12	136.53(19)	N8-Dy-N14	111.67(19)
N2-Dy-N14	83.2(2)	N9-Dy-N11	59.8(2)
N4-Dy-N5	149.16(19)	N9-Dy-N12	122.7(2)
N4-Dy-N7	134.4(2)	N9-Dy-N14	147.9(2)
N4-Dy-N8	67.7(2)	N11-Dy-N12	149.42(19)
N4-Dy-N9	75.19(19)	N11-Dy-N14	136.1(2)
N4-Dy-N11	122.68(19)	N12-Dy-N14	60.7(2)
N4-Dy-N12	84.10(19)		

Table S3. Selected bond lengths (Å) and bond angles (°) for **2**.

	Length(Å)		Length(Å)
Er-N1	2.539(4)	Er-N8	2.547(4)
Er-N2	2.499(4)	Er-N9	2.536(4)
Er-N4	2.543(4)	Er-N11	2.594(4)
Er-N5	2.527(4)	Er-N12	2.527(4)
Er-N7	2.559(4)	Er-N14	2.556(4)
	Angle(°)		Angle(°)
N1-Er-N2	61.7(1)	N4-Er-N14	73.2(1)
N1-Er-N4	113.1(1)	N5-Er-N7	60.8(1)
N1-Er-N5	61.8(1)	N5-Er-N8	117.0(1)
N1-Er-N7	112.7(1)	N5-Er-N9	135.3(1)
N1-Er-N8	178.7(1)	N5-Er-N11	84.2(1)
N1-Er-N9	119.5(1)	N5-Er-N12	73.8(1)
N1-Er-N11	68.0(1)	N5-Er-N14	77.2(1)
N1-Er-N12	117.5(1)	N7-Er-N8	66.6(1)
N1-Er-N14	67.9(1)	N7-Er-N9	82.4(1)
N2-Er-N4	61.6(1)	N7-Er-N11	74.3(1)
N2-Er-N5	123.4(1)	N7-Er-N12	75.6(1)
N2-Er-N7	147.4(1)	N7-Er-N14	126.2(1)
N2-Er-N8	119.6(1)	N8-Er-N9	61.5(1)
N2-Er-N9	75.2(1)	N8-Er-N11	112.5(1)
N2-Er-N11	74.2(1)	N8-Er-N12	61.5(1)
N2-Er-N12	136.7(1)	N8-Er-N14	111.7(1)
N2-Er-N14	83.2(1)	N9-Er-N11	60.6(1)
N4-Er-N5	149.0(1)	N9-Er-N12	123.0(1)
N4-Er-N7	134.2(1)	N9-Er-N14	147.3(1)
N4-Er-N8	67.7(1)	N11-Er-N12	148.7(1)
N4-Er-N9	75.1(1)	N11-Er-N14	135.8(1)
N4-Er-N11	123.7(1)	N12-Er-N14	60.8(1)
N4-Er-N12	84.1(1)		

Table S4. Lanthanide geometry analysis by using Continuous Shape Measurements (CShM).[a]

Complex	*JBC (D_{4d})	JSP (C_{2v})	TD (C_{2v})
1	3.335	3.542	4.333
2	3.267	3.493	4.312

* JBC = bicapped square antiprism; JSP= sphenocorona; TD = tetradecahedron.

[a] (a) S. Alvarez, P. Alemany, D.Casanova, J. Cirera, M. Llunell and D. Avnir, *Coord. Chem. Rev*., 2005, **249**, 1693; (26) D. Casanova, M. Llunell, P. Alemany and S. Alvarez, *Chem. Eur. J.*, 2005, **11**, 1479.

Table S5. Energy levels and eigenstates for compounds **1** and **2** obtained from the fitting of the $\chi_m T$-T and M-H data simultaneously.

	Energy / cm^{-1}	Eigenstate
1	0	79%$\vert \mp 1/2\rangle$ + 18%$\vert \pm 3/2\rangle$ + 3%$\vert \mp 5/2\rangle$ +…
	72	79%$\vert \mp 3/2\rangle$ + 19%$\vert \pm 1/2\rangle$ + 2%$\vert \pm 5/2\rangle$ +…
	159	94%$\vert \mp 5/2\rangle$ + 4%$\vert \pm 3/2\rangle$ + 1%$\vert \pm 1/2\rangle$ +…
	290	99%$\vert \pm 7/2\rangle$ +…
	470	61%$\vert \pm 9/2\rangle$ + 38%$\vert \mp 9/2\rangle$ + …
	689	99%$\vert \pm 11/2\rangle$ +…
	973	84%$\vert \pm 13/2\rangle$ + 15%$\vert \pm 13/2\rangle$ + …
	1290	100%$\vert \pm 15/2\rangle$ +…
2	0	46%$\vert \pm 15/2\rangle$ + 44%$\vert \pm 11/2\rangle$ + 10%$\vert \pm 7/2\rangle$ +…
	166	53%$\vert \pm 13/2\rangle$ + 41%$\vert \pm 9/2\rangle$ + 3%$\vert \pm 5/2\rangle$ +…
	361	41%$\vert \mp 1/2\rangle$ + 32%$\vert \pm 3/2\rangle$ + 19%$\vert \mp 5/2\rangle$ +…
	915	54%$\vert \pm 7/2\rangle$ + 32%$\vert \pm 15/2\rangle$ + 7%$\vert \mp 5/2\rangle$ +…
	1204	57%$\vert \pm 5/2\rangle$ + 27%$\vert \mp 3/2\rangle$ + 6%$\vert \pm 13/2\rangle$ +…
	1438	38%$\vert \pm 9/2\rangle$ + 31%$\vert \pm 13/2\rangle$ + 11%$\vert \mp 3/2\rangle$ +…
	1598	44%$\vert \pm 11/2\rangle$ + 29%$\vert \pm 7/2\rangle$ + 15%$\vert \pm 15/2\rangle$ +…
	1692	32%$\vert \pm 1/2\rangle$ + 14%$\vert \mp 3/2\rangle$ + 16%$\vert \mp 1/2\rangle$ +…